JACS
JOURNAL OF THE AMERICAN CHEMICAL SOCIETY
Communication
pubs.acs.org/JACS

Characterization and Carbohydrate Specificity of Pradimicin S

Syed Shahzad-ul-Hussan,[†] Rodolfo Ghirlando,[‡] Cajetan I. Dogo-Isonagie,[†] Yasuhiro Igarashi,[§] Jan Balzarini,[∥] and Carole A. Bewley*,[†]

[†]Laboratory of Bioorganic Chemistry and [‡]Laboratory of Molecular Biology, National Institute of Diabetes and Digestive and Kidney Diseases, National Institutes of Health, Bethesda, Maryland 20892, United States

[§]Biotechnology Research Center, Toyama Prefectural University, 5180 Kurokawa, Imizu, Toyama 939-0398, Japan

[∥]Rega Institute for Medical Research, Katholieke Universiteit Leuven, Leuven, Belgium

Supporting Information

ABSTRACT: The pradimicin family of antibiotics is attracting attention due to its anti-infective properties and as a model for understanding the requirements for carbohydrate recognition by small molecules. Members of the pradimicin family are unique among natural products in their ability to bind sugars in a Ca^{2+}-dependent manner, but the oligomerization to insoluble aggregates that occurs upon Ca^{2+} binding has prevented detailed characterization of their carbohydrate specificity and biologically relevant form. Here we take advantage of the water solubility of pradimicin S (PRM-S), a sulfated glucose-containing analogue of pradimicin A (PRM-A), to show by NMR spectroscopy and analytical ultracentrifugation that at biologically relevant concentrations, PRM-S binds Ca^{2+} to form a tetrameric species that selectively binds and engulfs the trisaccharide Manα1−3(Manα1−6)Man over mannose or mannobiose. In functional HIV-1 entry assays, IC_{50} values of 2−4 μM for PRM-S corrrelate with the concentrations at which oligomerization occurs as well as the affinities with which PRM-S binds the HIV surface envelope glycoprotein gp120. Together these data reveal the biologically active form of PRM-S, provide an explanation for previous speculations that PRM-A may contain a second mannose binding site, and expand our understanding of the characteristics that can engender a small molecule with the ability to function as a carbohydrate receptor.

Pradimicin S (**1**, PRM-S)[1,2] is a water-soluble, sulfated analogue of pradimicin A (**2**, PRM-A),[3] an antibiotic that exhibits in vivo antifungal activity, and is an entry inhibitor of HIV-1[4] and hepatitis C viruses.[5] In addition to their potent anti-infective activities, PRM-S and PRM-A have attracted much interest because they represent rare examples of nonpeptidic, small molecules with lectin-like properties.[6−8] PRM-A has been reported to oligomerize into large insoluble aggregates and to bind D-mannose with millimolar equilibrium dissociation constants (K_D's) in a Ca^{2+}-dependent manner.[9] Although a high-resolution structure of a pradimicin−carbohydrate complex would provide unmatched insight into carbohydrate recognition by a small organic molecule, the propensity of all pradimicins to form solid aggregates has thwarted such efforts. The increased solubility of PRM-S over other pradimicin family members provided us with an opportunity to study pradimicin assembly and carbohydrate recognition under physiological conditions, and determine how these properties relate to their biological activity. To accomplish this, we used an integrated approach employing analytical ultracentrifugation and NMR spectroscopy coupled with cell-based neutralization assays to characterize the Ca^{2+}-bound oligomerization of PRM-S, determine its carbohydrate specificity and identify carbohydrate atoms involved in PRM-S binding, and correlate the physical properties of PRM-S with its inhibitory activity in functional HIV-1 neutralization assays. We found that IC_{50} values coincide with conditions at which oligomerization occurs and the affinities with which PRM-S binds the HIV surface envelope glycoprotein gp120.

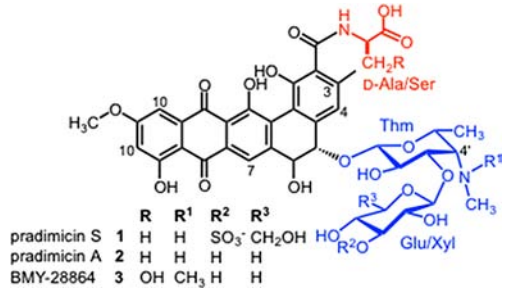

The chemical structure of PRM-S is composed of a benzo[*a*]naphthacenequinone aglycon, a D-Ala amino acid, and the disaccharide 3′-*O*-sulfo-β-D-glucosyl-β-D-thomosamine. In the presence of Ca^{2+}, pradimicins have been shown to form insoluble, solid aggregates; however, physical studies to date have been performed primarily with millimolar samples of pradimicins,[9,10] concentrations that exceed by orders of magnitude those at which their biological activities occur. To determine whether PRM-S is able to form discrete oligomeric structures at biologically relevant concentrations and in the presence of Ca^{2+}, we used analytical ultracentrifugation on a series of samples where the concentration of PRM-S ranged from approximately 10 to 40 μM (details appear in the Supporting Information [SI]). The sedimentation velocity data in Figure 1A show that in the absence of Ca^{2+}, PRM-S exists as a single monodisperse species whose sedimentation coefficient

Received: April 22, 2012
Published: July 11, 2012

   dx.doi.org/10.1021/ja303860m | *J. Am. Chem. Soc.* 2012, 134, 12346−12349

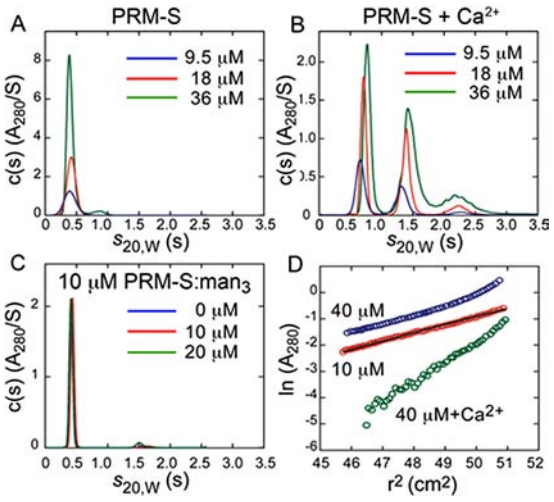

Figure 1. Characterization of PRM-S by analytical ultracentrifugation. Panels A–C show sedimentation velocity data of PRM-S in (A) the absence and (B) the presence of 5 mM $CaCl_2$ at loading concentrations of 9.5 (blue), 18 (red), and 36 μM (green). (C) Sedimentation velocity data of 10 μM PRM-S in the presence of 0 (blue), 10 (red), and 20 μM (green) mannotriose. Best fits of the data in the absence of Ca^{2+} and absence of Ca^{2+}/presence of mannotriose yield a molecular mass of 950 ± 15 g mol^{-1} corresponding to that of a PRM-S monomer. In the presence of $CaCl_2$ (B), discrete higher-molecular mass PRM-S species are observed, the most prominent of which corresponds to a PRM-S oligomer with a molecular mass of 3350 ± 60 g mol^{-1}. (D) Sedimentation equilbrium data of 10 μM (red) and 40 μM (blue) PRM-S in the absence of Ca^{2+}, and 10 μM PRM-S in the presence of 5 mM $CaCl_2$ (green). The superposed black line shows the expected slope for monomeric PRM-S. Data collected at 60,000 rpm are plotted in terms of the natural log of the absorbance against the radius-squared (r^2) to illustrate the degree of PRM-S association.

(0.41 S) corresponds to a molecular mass of 950 ± 15 g mol^{-1}, in excellent agreement with the molecular mass of PRM-S (948.9 g mol^{-1}). When excess Ca^{2+} is added to the solutions, a series of discrete species that accumulates sediment significantly faster than the monomer (Figure 1B). At the lowest loading concentration (9.5 μM), only two species are observed: the slowest sedimenting and most abundant species at 0.67 S has a best-fit molar mass of 3350 ± 60 g mol^{-1}, while the minor species at 1.32 S is significantly larger and has an estimated mass of 9300 ± 290 g mol^{-1} (SI, Figure S1). The ultracentrifugation data show that higher-molecular weight species become more prominent as the concentration of PRM-S is increased (Figure 1B), but this species comprises a very small component of the solution at low micromolar concentrations (SI, Figure S1). (Indeed, we were unable to detect the presence of large particles by dynamic light scattering at these concentrations [data not shown].) Together, these data demonstrate that, even in the presence of Ca^{2+}, PRM-S can form discrete, soluble oligomers in solution at low micromolar concentrations.

To determine whether, in the absence of Ca^{2+}, the carbohydrate ligands alone can induce PRM-S association, sedimentation velocity data were measured on solutions containing only PRM-S and Manα1–3(Manα1–6)Man (see below). As seen in Figure 1C, the data are comparable to those of PRM-S in the absence of Ca^{2+} demonstrating that carbohydrate alone does not induce PRM-S oligomerization. Last, to confirm the observations made by sedimentation velocity data, sedimentation equilibrium experiments were carried out on PRM-S solutions in the absence or presence of 5 mM $CaCl_2$ (Figure 1D). Best fits of the data confirm that apo-PRM-S and Ca^{2+}-bound PRM-S are present as a monodisperse monomer and oligomer, respectively (SI).

We took advantage of the water solubility of PRM-S by using ^{1}H NMR to further investigate the individual effects of Ca^{2+}, carbohydrate, and PRM-S concentration on the oligomerization of PRM-S under physiological conditions. ^{1}H NMR spectra were recorded on samples containing 5, 10, 20, and 50 μM PRM-S in D_2O (pH 6.85). As seen in Figure S2 (SI), each spectrum showed the presence of sharp ^{1}H signals for PRM-S indicating the existence of a single low-molecular weight species and overall absence of aggregation under these conditions, consistent with the analytical ultracentrifugation data. By comparison, in aqueous solutions of PRM-A prepared at similar concentrations and under identical conditions, we observed immediate formation of insoluble aggregates that precipitated from solution, and the ^{1}H NMR spectra of those samples consisted solely of broadened peaks (SI Figure S3).

PRM-S and PRM-A were recently shown to be HIV-1 entry inhibitors that act at the early stage of virus infection, presumably through interactions with oligomannosides present on the viral envelope glycoprotein gp120.[11] We sought to determine the carbohydrate specificity of PRM-S using saturation transfer difference (STD) NMR[12] combined with a fragment-based approach employing di– and trisaccharide components of high mannose oligosaccharides (Figure S4, SI). STD NMR is a powerful technique that is routinely used to define precise binding epitopes on small molecule ligands by way of NMR relaxation. The method requires samples comprising a large molecular weight receptor (~10 kDa or larger) in the presence of an excess of ligand (~50–100–fold). Mindful of the ultracentrifugation data, we recorded STD NMR spectra of synthetic fragments of oligomannose in the presence of 50 μM PRM-S and Ca^{2+}, conditions at which oligomeric species larger than 10 kDa are present (Figure 1B). As seen in the STD NMR spectrum in Figure 2A, in the presence of PRM-S–Ca^{2+} we observed remarkably strong enhancements for the trisaccharide core Manα1–3(Manα1–6)Man (mannotriose) with approximately equal intensities for the majority of the protons present (SI, Table S1). Although spectral overlap did not allow us to integrate individual peaks of the mannotriose difference spectrum, the degree of enhancements indicate that the trisaccharide is nearly completely surrounded by the pradimicin oligomer. Significantly reduced binding was observed for the terminal disaccharide Manα(1–2)Man (Figure 2B), and binding to Man-*O*-Me was too weak to be detected by solution NMR (Figure 2C). No binding was observed to the core structure $GlcNAc_2$ (Figure S4, SI). Thus, PRM-S shows remarkable specificity for the mannotriose core present of *N*-linked oligomannosides.

The surface envelope glycoprotein of HIV, gp120, is distinguished by its dense display of complex carbohydrates, where an abundance of high mannose oligosaccharides is present.[13,14] The carbohydrate-binding properties of the pradimicins engender these small molecules with the ability to inhibit HIV-1 entry through carbohydrate-mediated interactions with the viral envelope glycoprotein gp120. As with many carbohydrate-mediated HIV-1 entry inhibitors, the mode of binding of PRM-S to gp120 has not been defined, nor has the effect of oligomerization on antiviral activity. To examine the kinetics of binding of PRM-S to gp120 we used

dx.doi.org/10.1021/ja303860m | J. Am. Chem. Soc. 2012, 134, 12346–12349

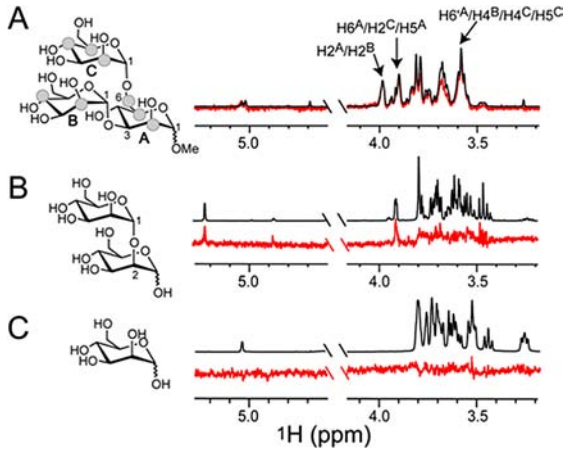

Figure 2. Carbohydrate specificity of PRM-S by STD NMR. Spectra were recorded on samples containing 50 μM PRM-S, 1 mM $CaCl_2$, and 1 mM (A) Manα1−3(Manα1−6)Man, (B) Manα(1−2)Man, or (C) Man-*O*-Me with identical acquisition parameters (SI). Difference spectra (red) are superimposed (A) or shown below (B,C) their corresponding reference spectra (black). Strong enhancements are observed for virtually all protons of mannotriose. Signals showing the strongest enhancements and used for normalization are labeled and depicted as gray spheres. Enhancements for mannobiose are weak in comparison, and binding to mannose could not be detected.

surface Plasmon resonance where soluble gp120 (HIV-1 strain HXB2) was immobilized to the surface, and serial dilutions of PRM-S in the presence and absence of Ca^{2+} were analyzed for binding. To obtain excellent quality data, it was necessary to determine empirically the amount of gp120 to be immobilized onto the surface (details provided in the SI). As seen in Figure 3A, the data fit well to a heterogeneous ligand model with K_D

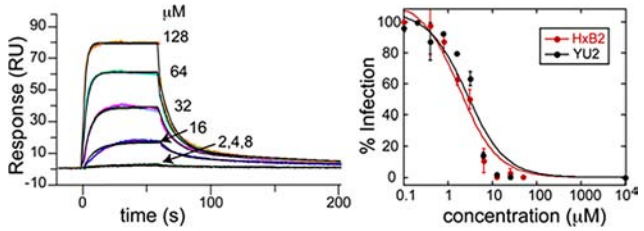

Figure 3. PRM-S binds HIV-1 gp120 and inhibits HIV-1 entry. (A) Binding of PRM-S to gp120 in the presence of Ca^{2+} measured by surface Plasmon resonance. (B) Inhibition curves for PRM-S toward HIV-1 strains HxB2 and YU2 obtained from HIV-1 infectivity assays. IC_{50} values are on the order of 2−4 μM, consistent with the K_D values of pradS/Ca^{2+} binding to gp120.

values of 2 and 32 μM (SI, Table S2). In the absence of Ca^{2+}, we did not observe binding to gp120 at any of the concentrations tested.

To characterize the active form of PRM-S that is capable of inhibiting viral entry, we tested our characterized PRM-S solutions in single round HIV-1 infectivity assays[15] using two different HIV-1 strains (including the CXCR4-using strain HXB2 and the CCR5-using strain YU2, SI). As seen in Figure 3B, PRM-S gave similar dose−response curves for both HIV-1 strains, with IC_{50} values around 2−4 μM, comparable to values reported for other pradimicins toward HIV-1.[4,11] Our surface Plasmon resonance results showed clearly that in the absence of Ca^{2+}, PRM-S is unable to bind gp120 in vitro. Because of the cellular requirement for Ca^{2+} and the duration of the neutralization assay (72 h), it is not possible to perform an analogous Ca^{2+}-free HIV-1 entry assay. However, our combined data indicate that during neutralization, PRM-S exists as a discrete monodisperse species when binding to virus-associated gp120, and the IC_{50} values for inhibitory activity correlate with concentrations at which Ca^{2+}-dependent tetramer formation is observed.

In this study we present the first detailed characterizaion of a pradimicin in solution at biologically relevant concentrations. By using an integrated approach that included NMR, analytical ultracentrifugation, surface Plasmon resonance and viral neutralization assays, we conclusively demonstrated that PRM-S is able to form discrete Ca^{2+}-dependent oligomers at low micromolar concentrations, a characteristic that has yet to be demonstrated for other pradimicins. Further, these PRM-S:Ca^{2+} complexes show extremely high selectivity for the mannotriose core structure Manα1−6(Manα1−3)Man that is present in all high mannose oligosaccharides. Interestingly and in contrast to observations for PRM-A, PRM-S binding to *O*-methyl mannoside was so weak as to be virtually undectable by STD NMR, a technique that readily detects weak carbohydrate−receptor interactions having millimolar K_D values.[12,16,17] On this note, others have speculated that a second mannose-binding site may be present in the pradimicins,[9,18] and this would be consistent with the stronger binding observed here for mannotriose over mannose. A major difference among the pradimicins is the identity and number of sugar units present in each of the natural products. Thus, it is possible that the presence of the 3-sulfoglucosyl unit unique to PRM-S accounts for its specificity toward mannotriose. By employing an integrated approach to the study of other pradimicin-carbohydrate complexes, we are optimistic that we will learn more about the assembly and carbohydrate recognition that occurs within this family of antibiotics. In closing, these results expand our understanding of small molecule-based carbohydrate receptors, and reveal new structural features that may augment design of synthetic carbohydrate receptors.

■ ASSOCIATED CONTENT

Ⓢ Supporting Information

General experimental methods; two tables and four figures. This material is available free of charge via the Internet at http://pubs.acs.org.

■ AUTHOR INFORMATION

Corresponding Author

*E-mail: caroleb@mail.nih.gov

Notes

The authors declare no competing financial interest.

■ ACKNOWLEDGMENTS

This work was supported in part by the Intramural Research Program of the National Institutes of Health (NIDDK), and KU Leuven, PF-10/18 (J.B.). C.D.-I. is a recipient of an Intramural AIDS Research Fellow award, Office of the Director, NIH.

■ REFERENCES

(1) Saitoh, K.; Tenmyo, O.; Yamamoto, S.; Furumai, T.; Oki, T. *J. Antibiot. (Tokyo)* **1993**, *46*, 580.

(2) Saitoh, K.; Tsuno, T.; Kakushima, M.; Hatori, M.; Furumai, T.; Oki, T. *J. Antibiot. (Tokyo)* **1993**, *46*, 406.

(3) Oki, T.; Konishi, M.; Tomatsu, K.; Tomita, K.; Saitoh, K.; Tsunakawa, M.; Nishio, M.; Miyaki, T.; Kawaguchi, H. *J. Antibiot. (Tokyo)* **1988**, *41*, 1701.
(4) Tanabe, A.; Nakashima, H.; Yoshida, O.; Yamamoto, N.; Tenmyo, O.; Oki, T. *J. Antibiot. (Tokyo)* **1988**, *41*, 1708.
(5) Bertaux, C.; Daelemans, D.; Meertens, L.; Cormier, E. G.; Reinus, J. F.; Peumans, W. J.; Van Damme, E. J.; Igarashi, Y.; Oki, T.; Schols, D.; Dragic, T.; Balzarini, J. *Virology* **2007**, *366*, 40.
(6) Davis, A. P.; James, T. D. In *Functional Synthetic Receptors*; Schrader, T., Hamilton, A. D., Eds.; Wiley-VCH: Weinheim, 2005.
(7) Mazik, M. *RSC Adv.* **2012**, *2*, 2630.
(8) Ueki, T.; Numata, K.; Sawada, Y.; Nakajima, T.; Fukagawa, Y.; Oki, T. *J. Antibiot. (Tokyo)* **1993**, *46*, 149.
(9) Nakagawa, Y.; Doi, T.; Masuda, Y.; Takegoshi, K.; Igarashi, Y.; Ito, Y. *J. Am. Chem. Soc.* **2011**, *133*, 17485.
(10) Nakagawa, Y.; Masuda, Y.; Yamada, K.; Doi, T.; Takegoshi, K.; Igarashi, Y.; Ito, Y. *Angew. Chem., Int. Ed.* **2011**, *50*, 6084.
(11) Balzarini, J.; Francois, K. O.; Van Laethem, K.; Hoorelbeke, B.; Renders, M.; Auwerx, J.; Liekens, S.; Oki, T.; Igarashi, Y.; Schols, D. *Antimicrob. Agents Chemother.* **2010**, *54*, 1425.
(12) Mayer, M.; Meyer, B. *Angew. Chem., Int. Ed.* **1999**, *38*, 1784.
(13) Doores, K. J.; Bonomelli, C.; Harvey, D. J.; Vasiljevic, S.; Dwek, R. A.; Burton, D. R.; Crispin, M.; Scanlan, C. N. *Proc. Natl. Acad. Sci. U.S.A.* **2010**, *107*, 13800.
(14) Go, E. P.; Chang, Q.; Liao, H. X.; Sutherland, L. L.; Alam, S. M.; Haynes, B. F.; Desaire, H. *J Proteome Res.* **2009**, *8*, 4231.
(15) Li, M.; Gao, F.; Mascola, J. R.; Stamatatos, L.; Polonis, V. R.; Koutsoukos, M.; Voss, G.; Goepfert, P.; Gilbert, P.; Greene, K. M.; Bilska, M.; Kothe, D. L.; Salazar-Gonzalez, J. F.; Wei, X.; Decker, J. M.; Hahn, B. H.; Montefiori, D. C. *J. Virol.* **2005**, *79*, 10108.
(16) Hansman, G. S.; Shahzad-Ul-Hussan, S.; McLellan, J. S.; Chuang, G. Y.; Georgiev, I.; Shimoike, T.; Katayama, K.; Bewley, C. A.; Kwong, P. D. *J. Virol.* **2012**, *86*, 284.
(17) McLellan, J. S.; Pancera, M.; Carrico, C.; Gorman, J.; Julien, J. P.; Khayat, R.; Louder, R.; Pejchal, R.; Sastry, M.; Dai, K.; O'Dell, S.; Patel, N.; Shahzad-ul-Hussan, S.; Yang, Y.; Zhang, B.; Zhou, T.; Zhu, J.; Boyington, J. C.; Chuang, G. Y.; Diwanji, D.; Georgiev, I.; Kwon, Y. D.; Lee, D.; Louder, M. K.; Moquin, S.; Schmidt, S. D.; Yang, Z. Y.; Bonsignori, M.; Crump, J. A.; Kapiga, S. H.; Sam, N. E.; Haynes, B. F.; Burton, D. R.; Koff, W. C.; Walker, L. M.; Phogat, S.; Wyatt, R.; Orwenyo, J.; Wang, L. X.; Arthos, J.; Bewley, C. A.; Mascola, J. R.; Nabel, G. J.; Schief, W. R.; Ward, A. B.; Wilson, I. A.; Kwong, P. D. *Nature* **2011**, *480*, 336.
(18) Fujikawa, K.; Tsukamoto, Y.; Oki, T.; Lee, Y. C. *Glycobiology* **1998**, *8*, 407.